Topography orientation effects on friction and wear in sliding DLC and steel contacts, part 3: Experiments under dry and lubricated conditions

K. Holmberg [a,*], A. Laukkanen [a], T. Hakala [a], H. Ronkainen [a], T. Suhonen [a], M. Wolski [b],
P. Podsiadlo [b], T. Woloszynski [b], G. Stachowiak [b], C. Gachot [c], L. Li [d]

[a] *VTT Technical Research Centre of Finland, Espoo, Finland*
[b] *Curtin University, Perth, Australia*
[c] *TU Wien, Austria*
[d] *City University of Hong Kong, Hong Kong*

ARTICLE INFO

ABSTRACT

Surface topography can affect the tribological performance in many applications. The influence of surface roughness and topographic orientation on friction and wear in dry and oil lubricated steel vs steel and diamond-like carbon (DLC) coated steel vs DLC coated steel sliding contacts was investigated. The surfaces had a centerline average roughness (R_a) between 0.004 and 0.11 μm and a topographic groove orientation of 0°, 45° and 90° with respect to the sliding direction. Tests conducted showed that the strongest effect of the orientation of the topographic directions occurs in dry sliding DLC vs DLC contacts. A super-lubricious DLC surface layer was efficiently formed, exhibiting low friction coefficients of 0.04 for smooth surfaces, and rough surfaces with grooves oriented along the sliding direction. The process of surface layer formation was most severely disturbed for average surfaces roughness with grooves oriented at 45° to the sliding direction. For these surfaces, the coefficient of friction was about five times higher (0.21) as compared to smooth samples (0.04). In dry sliding steel contacts, the coefficient of friction decreased with increasing surface roughness. On the other hand, the coefficient of friction increased with surface roughness in oil lubricated steel contacts. Adding a synthetic oil into the DLC vs DLC sliding contact prevented the formation of the super-lubricious surface layer. In tests with rotational steel vs steel sliding the friction coefficient was about 10% lower than in test with linear reciprocal sliding but was higher in DLC vs DLC contacts.

1. Introduction

The effect of friction and wear on energy use, environment and economy has recently been calculated in a series of studies conducted by Holmberg et al. [1–4]. The studies showed that 23% of the world's total energy consumption is wasted in tribological contacts. Out of that 20% is used to overcome friction and 3% is used to remanufacture worn parts and replacement equipment due to wear and wear-related failures. In some industrial areas, like in mining industry, as much as 40% of the consumed energy is used to overcome friction and the economic losses caused by wear are significant. Globally friction and wear are responsible for 8120 million tons of CO_2 emissions per year. It is thus imperative to find new technological means to reduce both friction and wear in industrial and other applications used by our society for economic and energy saving reasons, and also in light of the ongoing climate change

issues.

Over the last fifty years tribological contact mechanisms have been extensively studied; theoretically, experimentally, application related and on scales all from macroscale down to nanoscale [5–7]. In tribo-contacts friction is often better understood than wear processes occurring which in many cases are more complex and difficult to describe and also to model. The contact mechanisms become even more complex when the surfaces are modified, e.g., coated, in order to reduce friction and wear. Thin surface coatings, such as hard ceramic or very lubricious carbon-based coatings, as well as thicker composite coatings, have successfully been applied in a great number of applications [8].

Often, for simplicity, surfaces in tribocontacts studied are often assumed to be smooth. However, in reality they always exhibit some topographic pattern influencing the shear plane at the contact where both friction and wear take place. In dry contacts, elastically or

plastically deformed surface asperities will influence the real contact area [6,9–11]. The form and orientation of asperities can affect the lubricant flow and generation of partial hydrodynamic forces acting between the asperities in lubricated contacts [12]. Typical industrial applications where the surface roughness has an important effect on friction and wear are the cylinder liners in heavy duty diesel engines. Typically, the cast iron cylinder liners are honed in order to induce smooth surfaces with deep valleys. These valleys act as lubricant reservoirs. The smoothness of the surfaces between the valleys has been found to result in a quicker formation of protecting tribofilm and generation of low initial real contact pressure [13].

Diamond-like carbon (DLC) coatings have been largely investigated during the last three decades due to their excellent tribological properties in machine components and in manufacturing [8]. These includes lubricated contacts, influenced by the interactions between the base oil structure, lubricant additive chemistry and doped materials in DLC coatings [14–16]. There have been a number of studies on the influence of surface roughness on friction and wear in DLC coated surface contacts. However, the results are still not clear and sometimes even contradictory, probably, at least partly, due to differences in the structures of DLC coatings investigated. Different mechanical response to loading and varying tribochemical effects have been reported [17–20]. An increase in wear is often reported for higher surface roughness.

Surface texturing is the technique used to intentionally modify the surface topography by introducing well-defined dimples, pockets, grooves or protrusions of various shapes and configurations. This can be done on macro scale by machining the surface, on micro scale by, e.g., laser-based texturing and on nano scale by, e.g., lithographic techniques developed for micro-electro-mechanical-systems (MEMS) and nano-electronics [21–23]. These new surface manufacturing techniques, better understanding of the basic contact mechanisms, novel surface characterization methods and contact modelling allow for the development of new tools for optimization of the tribological performance of textured surfaces [23–25]. The synergistic effects of surface textures and solid lubricants to tailor friction and wear have been studied [62].

Surface texturing has been most beneficial in cases of conformal contacts with parallel sliding and full film lubrication [26,27]. Friction reduction has also been reported in mixed and boundary lubricated regimes, and to a lesser degree in hydrodynamic lubrication [23,28,29]. The combination of surface texturing in the form of dimples combined with a DLC coating deposited on the cylinder surfaces of a motorcycle improved tribological performance and increased a maximum power output by up to 5.8% [30]. A computational method for analyzing the combined effect of surface roughness and coating's mechanical properties in elasto-hydrodynamic lubricated contacts of spur gears with regard to contact performance, film thickness, friction and surface stress field was developed and showed a significant effect of surface roughness [31].

The influence of surface roughness in tribological contacts was early recognized [9,10,32,33] and has been utilized in various industrial applications [34,35]. Standard surface characterization parameter, i.e., the centerline average value (R_a) is a commonly used measure of surface roughness used in shop floor engineering. However, the commonly used, standard parameters have considerable limitations [36], i.e., they tend to work well only with isotropic surfaces and are not able to provide detailed information about surface's anisotropy and roughness at different scales of measurement. This is important, because topography of engineering surfaces, including DLC coated, exhibit multi-scale and anisotropic nature [37–39]. This means that surface topography characteristics changes with scale and direction of measurement.

The influence of surface roughness or surface pattern orientation with regard to sliding direction has been the subject of only very few investigations and the results obtained are not straightforward. This is probably due to the difficulty in defining and controlling the several different and competing contact mechanisms which have effect on friction and wear. The main difficulties are associated with the lubrication transition mechanism from hydrodynamic to dry sliding, contact area and adhesion at dry contacts, surface pattern alignment, sliding speed, load, contact surface chemistry, scale effects, and detailed surface topography characterization.

It has been shown, when modelling the transition from hydrodynamic to boundary lubrication regimes at low lambda (λ) ratios, that the average film thickness in rough contacts is often slightly greater than in smooth contacts. The surface topography and orientation had noticeable effects on asperity contact area and load sharing, but they show limited influence on average film thickness. The film thickness seemed to be mostly determined by the conditions in the contact inlet region where surface roughness does not have much of the influence [40]. In boundary lubricated typical galling test conditions the effect of dimples as lubrication reservoirs has been shown but topographic effects in dry sliding were negligible [41].

Ball-on-plate experiments in dry sliding conducted in a linear reciprocating tribotester showed reduced friction when an un-patterned ball was sliding over perpendicular grooves compared to sliding over aligned grooves. Lower friction was measured when grooves on both plate and ball were perpendicular compared to surface with parallel grooves. In general, the patterned surfaces exhibited lower friction than the smooth reference surfaces [42].

Recent surface characterization methods allow for studying the effects of surface topographic features on friction and wear in greater details both experimentally and numerically [43–45] on micro and nano scales [19,46]. Some of the works also include the studies of the topographic orientation effects [23,40,42,47,48]. The influence of surface roughness on wear in DLC coated surfaces has also been demonstrated [17,49].

In our earlier works, we have conducted the experiments to investigate the influence of surface topography, especially the effects of topographic orientation on steel vs steel and DLC vs DLC coated surfaces under dry sliding conditions [50,51]. We have also conducted computer simulations and modelling using the same contact conditions [52,53]. The steel and DLC coated surfaces have been characterized using variance orientation transform (VOT) method [50,53]. The VOT method calculates fractal signatures (FS, sets of fractal dimensions) in different directions, and at individual scales. We found that the VOT provides vital information about surface roughness and anisotropy which can be used in analysis of surfaces, also in steel vs steel and DLC vs DLC coated contacts. The simulations showed a significant influence of the topographic orientation on the stress-strain state within the roughness peaks and thus on the local tensile stresses resulting in local cracking and wear. The surface structure was up to four times more rigid in the direction of grooves as compared to the flexible behavior in the perpendicular direction. The macro topography dominated the tendency for surface cracking and plastic deformation which in turn, was influencing wear and friction. The micro-topographical features contributed to cracking and deformation by less than 40%.

The current study is a continuation of our previous work by extending the scope to oil lubricated contacts. The same materials and characterization data of topographies and mechanical properties are used. In this work, we compare friction and wear performance with respect to surface roughness and topographic orientation for both dry and oil lubricated surfaces, and also to explore the basic tribological contact mechanisms involved.

2. Methodology

The approach we use in this work is Process-Structure-Properties-Performance (PSPP) presented in detail in by Holmberg et al. [54,55]. Detailed description of micro scale of microstructural and micro-topographic features of the sample surfaces and tribological experiments, i.e., linear reciprocating ball-on-plate and rotational ball-on-disc sliding, is included. As the results for dry sliding have previously been reported [50] they are only partially included where the

comparison with lubricated conditions is required. In order to better understand the physical contact mechanisms influencing friction and wear we have modelled the contact conditions using finite elements method. We also conducted computer simulations of microscale sliding using the empirical contact conditions. The computational results will be reported separately as part four of this series of articles.

3. Materials and their mechanical properties

Discs of bearing steel (AISI52100) with three different roughness levels common in engineering applications were investigated. The discs were heat treated to 6.3 GPa hardness. On some of the discs a hydrogen-free amorphous diamond-like carbon (DLC a-C) coating was deposited by physical vapor deposition (PVD) magnetron sputtering technique. This was a Graphite-IC variant rooted from the non-hydrogenated DLC coatings developed by Dennis Teer [50,71,73,74]. The DLC coating had a multilayer structure. Attached to the substrate surface on top of each other were Cr buffer, CrCx gradient and DLC layers, as shown in Fig. 1.

The steel samples were ground to give them a surface topography with oriented grooving. Two smoother surface finishes were produced by polishing the ground discs with two grades polish media. The ground surface was classified as rough (R), while the two polished surfaces as average rough (A) and smooth (S). The three-dimensional (3D) surface topography was measured by chromatic confocal surface profilometer and analyzed using the VOT method as described in our earlier work [50]. Using the VOT, FSs were calculated in three directions $0°$ (FS_0), $45°$ (FS_{45}) and $90°$ (FS_{90}) along with texture aspect ratio signature (StrS) at scales ranging from 0.36 to 0.84 mm 3D images of the surfaces tested are shown in Fig. 2.

The thickness of the individual coating layers was measured from FIB (focused ion beam) cross-section, using a dual beam SEM/FIB facility as shown in Fig. 1. The layers were analyzed in the SEM using electron spectroscopy. The layer's structure was practically homogenous, i.e., virtually free from microstructural features like pores, defects, etc. on sub-micron scale. Indentation tests were performed both at nano and macro scales, in order to assess the elastic and plastic behavior of the coated system and its constituent components.

The lubricant used in the experiments was pure, free of additives and contaminants, low molecular weight polymerized high viscosity poly-alpha-olefin (PAO) oil with 408 cSt viscosity at $+40\ °C$ and a viscosity index of 149. Details of the surface samples and the lubricant are summarized in Table 1.

The DLC coated steel plate and ball counter-surface differ in measured hardness. The difference is attributed to different scale hardness measurement techniques used (nano vs micro).

4. Experimental methods

The experiments were carried out using two different test configurations in order to gain information on sliding over the defined surface topography both in rotational and in linear directions, i.e., in unidirectional (ball-on-disc) and reciprocal sliding (ball-on-plate). The tests were carried out using an Anton Paar Tritec Ball-on-disk tribometer TRB[3] [64].

4.1. Linear reciprocating ball-on-plate tests

The ball used in ball-on-plate (BOP) tests was of 10 mm diameter steel ball with a roughness of R_a 0.01 μm, sliding in linear reciprocating movement over the test plate. The stroke was 0.01 m and the sliding speed was 0.01 m/s. The normal load was stepwise increased from 1 N to 20 N over a period of 10 min followed by continuous sliding at 20 N load for 20 min. The sliding was carried out in three directions, $0°$, $45°$ and $90°$ to sliding direction, see Fig. 3. Two or three test were repeated for each direction. The tests were conducted at room temperature of $22 \pm 1\ °C$ and a relative humidity of $50 \pm 5\%$.

4.2. Continuous unidirectional ball-on-disc tests

In ball-on-disc (BOD) tests, the same steel ball with a diameter ball of 10 mm and a roughness of R_a 0.01 μm was used. The sliding track had a diameter of about 30 mm while the sliding speed was 0.034 m/s. A normal load force of 20 N was applied and the sliding time was 3 h. The sliding friction was measured, and the wear rates were calculated accordingly using optical microscopy and 2D profilometry. The tests were conducted at room temperature of $22 \pm 1\ °C$ and a relative humidity of $50 \pm 5\%$. A few dry low-speed tests with a sliding speed of 0.01 m/s were carried out in order to obtain results with same speed that was used in the BOP testing for comparison.

5. Experimental results

As already mentioned two sets of tests were carried out. During ball-on-disc tests, described in section 4.2, the sliding direction was continuously changing with each rotational cycle of $360°$. In this case, the effects of topography orientation could not be determined from the results. For this reason, a second set of tests was carried out with the same surfaces and under similar test conditions but using a reciprocal linear sliding test, as described in section 4.1.

The detailed test results are presented in Appendix 1 Tables A1 and A2 and they are also presented as graphs in Figs. 4, 5, 8, 9, 11 and 12 together with earlier results published for dry conditions [50]. Figs. 4 and 5 represent a summary of all test results. Results for different topographic orientations are presented only as average values. Figs. 8, 9, 11 and 12 show the results for the four topographic orientations investigated in DLC vs DLC dry and lubricated contacts. The impact on friction and wear of the following five key parameters:

- **surface material**: steel and DLC,
- **lubrication condition**: dry and oil lubricated,
- **surface roughness**: smooth, average rough and rough surface,
- **topographic orientation**: $0°$, $45°$ and $90°$, and
- **sliding direction**: reciprocal linear and continuous rotational,is shown.

Test results and observations are summarized below following the same order as they are presented in Figs. 4 and 5, in four parts from left
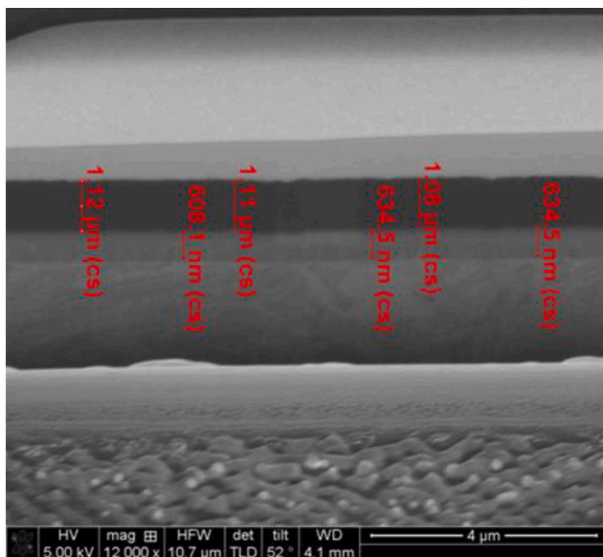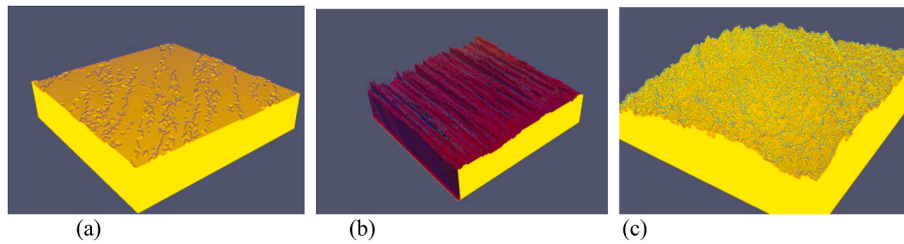

Fig. 1. Section of the smooth DLC coated surface showing from top the thickness of the DLC, CrCx gradient, and Cr buffer layers and the steel (AISI52100 100Cr6) substrate.

Fig. 2. Examples of 3D images of the steel surfaces (AISI52100 100Cr6) with three levels of surface roughness, (a) smooth surface with $R_a = 0.004$ μm, (b) average rough surface with $R_a = 0.01$ μm, and rough surface with $R_a = 0.1$ μm.

to right. Steel vs steel contacts, dry and lubricated, are first presented followed by DLC vs DLC contacts, dry and lubricated. The results are further discussed in Section 6. For the DLC vs DLC contacts more detailed results are presented in Figs. 8, 9, 11 and 12.

Similar graphs for the steel vs steel contacts have not been included as no clear topography effects could be observed. In dry sliding the surface topography pattern was quickly destroyed. Also in lubricated sliding no effect of topography orientation could be measured. This is demonstrated by both the wear scar and wear track images in Figs. 6 and 7 as well as by the data presented in Tables A1 and A2 in Annex 1.

5.1. Dry sliding with steel vs steel contacts, part one (Figs. 4 and 5)

High values of the friction coefficient of 0.65–0.72, were observed for smooth surface contacts ($R_a = 0.004$ μm) while for rougher surfaces (up to $R_a = 0.1$ μm) these values were lower, i.e., 0.51–0.57 in both linear and rotational sliding. In general, the friction coefficient was about 10% lower in rotational sliding compared to linear reciprocating sliding.

The sever wear conditions for steel vs steel dry sliding with four topography orientations with average surface roughness are shown in Fig. 6. The wear resulted in the formation a steel layer that inhibited the effect of topography pattern.

In linear siding both the smooth and the rough surfaces showed lower ball wear rates (28 and 23 $\cdot 10^{-6}$ mm^3/Nm) at 0° orientation and slightly increased wear (up to 31 and 33 $\cdot 10^{-6}$ mm^3/Nm) with 45° and 90° orientations. The average rough surface exhibited the highest wear rate (38 $\cdot 10^{-6}$ mm^3/Nm) at 0° orientation with decreasing rate (down to 28 $\cdot 10^{-6}$ mm^3/Nm) with 45° and 90° orientations.

The flat disc wear was in the range of 0.01–0.023 $\cdot 10^{-6}$ mm^3/Nm in linear sliding with smooth surfaces. Also, a layer formation with average and rough surfaces was observed.

During rotational sliding the wear rate of the ball was of the same order of magnitude as in linear sliding. The disc wear observed was low $<0.012 \cdot 10^{-6}$ mm^3/Nm. For details see Table 6 in [50].

5.2. Lubricated sliding with steel vs steel contacts, part two (Figs. 4 and 5)

The smooth surface yielded low coefficient of friction both in linear and rotational sliding (0.08 and 0.10 respectively). They increased with increasing surface roughness up to 0.13 for the rough surfaces in all sliding directions investigated. No influence of topographic orientation was observed.

The lubricant film protected the surfaces from wear so that the wear was in many cases hardly detectable, see Fig. 7. The surface of balls wore less than 0.01 $\cdot 10^{-6}$ mm^3/Nm in linear sliding. In rotational sliding, it showed a slightly increasing wear rate (from 0.01 to 0.04 $\cdot 10^{-6}$ mm^3/Nm) with surface roughness. Wear of the flat disc surface was hardly detectable ($<0.005 \cdot 10^{-6}$ mm^3/Nm). The topographic orientation and surface roughness had no considerable influence on wear.

5.3. Dry sliding with DLC vs DLC contacts, part three (Figs. 4 and 5)

The coefficient of friction for smooth surfaces ($R_a = 0.005$ μm) was extremely low of only 0.04 in linear sliding. The friction was equally low for the average and rough surfaces with 0° topography orientation. Slightly increased values of 0.05 and 0.07 for the two rougher surfaces and 90° orientation was recorded, see Fig. 8.

A noteworthy observation was made that the coefficient of friction was the highest, of 0.21, with average surface roughness and 45° orientation. For the 45° orientation and rough surface it was 0.12 for comparison. The coefficient friction, of 0.10–0.17, was clearly higher in rotational sliding with increasing roughness.

The ball wear rate was very low in linear sliding (0.005 $\cdot 10^{-6}$ mm^3/Nm) with smooth surfaces and increasing with surface roughness to 0.01 $\cdot 10^{-6}$ mm^3/Nm, see Fig. 9. The disc surface wear was hardly detectable ($<0.01 \cdot 10^{-6}$ mm^3/Nm), as can be seen in Fig. 10. The ball wear was also very low in rotational sliding with wear rates of only 0.01–0.08 $\cdot 10^{-6}$ mm^3/Nm and again increasing with surface roughness. The disc surface wear was hardly detectable ($<0.05 \cdot 10^{-6}$ mm^3/Nm). In both the linear and in rotational sliding with 45° topography orientation the DLC coating on the ball was worn out, see Fig. 10 b and d.

5.4. Lubricated sliding with DLC vs DLC contacts, part four (Figs. 4 and 5)

The coefficient of friction was in all cases studied between 0.07 and 0.10, see Fig. 11. In linear sliding the lower and higher values of the coefficient correspond to smooth surfaces and rough surfaces respectively.

The ball wear was very low in linear sliding (below 0.03 $\cdot 10^{-6}$ mm^3/Nm), see Figs. 12 and 13. The disc surface wear was hardly detectable ($<0.002 \cdot 10^{-6}$ mm^3/Nm). The ball wear was also very low in rotational sliding with wear rates of only 0.01–0.08 $\cdot 10^{-6}$ mm^3/Nm and again increasing with surface roughness while the disc surface wear was hardly detectable ($<0.002 \cdot 10^{-6}$ mm^3/Nm).

5.5. Friction in linear and rotational sliding, the speed effect

The difference in the friction and wear results measured in continuous rotational sliding with ball-on-disc and reciprocal linear sliding with ball-on-plate was both confusing and interesting. In order to find out if this could be due to the difference in sliding speed additional low-speed experiments with DLC vs DLC were carried out using the BOD test at the same sliding speed 0.01 m/s as used in the BOP test. The results obtained showed no significant difference in the coefficient of friction due to sliding speed. At a sliding speed of 0.034 m/s the friction coefficient was 0.10 ± 0.02 while at 0.01 m/s it was 0.11 ± 0.03. Friction measurements in similar test conditions carried out by Velkavrh and Kalin [16] also indicate only a minor influence of speed on friction within the range investigated.

Table 1
Details of surface samples and lubricant.

Properties	Symbol (unit)	DLC coatings	Steel samples and substrates
Flat plate surface		DLC coated steel disc	Uncoated steel disc
Surface material		Diamond-like carbon	AISI52100 (100Cr6)
Substrate material		AISI52100 (100Cr6) steel, see column to the right	–
Total coating thickness	h (μm)	1.76 ±0.04	–
Surface hardness (nano)	H (GPa)	18 ±1.3	6.3
Surface elastic modulus (nano)	E (GPa)	205 ±10	220
Surface Poisson's ratio	v (−)	0.202[a]	0.3[a]
Surface roughness			
- smooth	R_a (μm)	0.005	0.004
- average rough	R_a (μm)	0.01	0.01
- rough	R_a (μm)	0.11	0.1
Surface roughness VOT	Mean		
- smooth	$FS_0/FS_{45}/$	2.37/2.47/2.57/0.62	2.21/2.29/2.29/0.88
- average rough	$FS_{90}/StrS$	2.55/2.66/2.78/0.58	2.66/2.76/2.72/0.62
- rough		2.39/2.76/2.79/0.42	2.65/2.94/2.94/0.33
Yield strength	MPa	–	2100
Tensile strength	MPa	–	2300
Tangent modulus	GPa	–	22.0
Strain hardening exponent 1	N	–	20.0
Ball counter-surface		**DLC coated steel ball**	**Uncoated steel ball**
Surface material		Diamond-like carbon	AISI52100 (100Cr6)
Substrate material		AISI52100 (100Cr6) steel, see column to the right	–
Diameter	mm	10	10
Roughness	R_a (μm)	0.01	0.01
Surface hardness (micro)	H (GPa)	8	7
Surface elastic modulus (micro)	E (GPa)	206	220
Surface Poisson's ratio	v (−)	0.202[a]	0.3
Yield strength	MPa	–	2100
Tensile strength	MPa	–	2300
Strain hardening exp 1	N	–	20.0
Lubricant, Synton PAO40			
- viscosity at +40 °C	cSt	408	
-viscosity at +100 °C	cSt	40.5	
-viscosity-index	–	149	
-density at +15 °C	kg/m3	858	
-sulphur	ppm	11	
-additives	ppm	0	
-contamination	ppm	0	

[a] From literature.

6. Discussion

6.1. Analysis of friction and wear results from dry and lubricated experiments

Our objective was to investigate the effects on surface roughness and topographic orientation on friction and wear in dry and lubricated sliding. Four main contact mechanisms involved were observed as
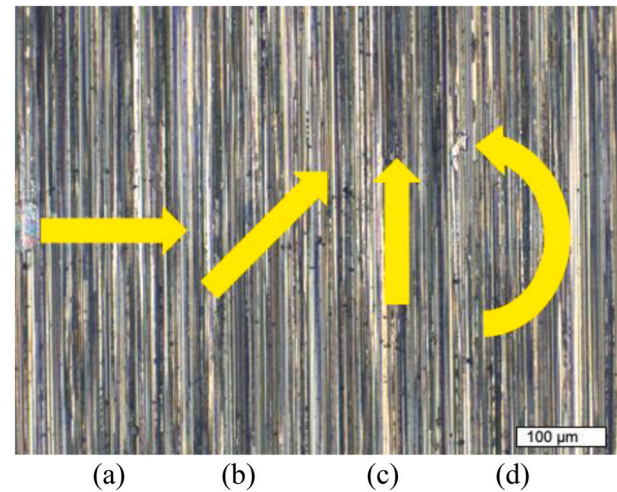

Fig. 3. The sliding directions in linear ball-on-plate tests (a) perpendicular 90°, (b) 45°, and (c) parallel 0°, and in rotational ball-on-disc tests (d) 0°–360° continuous unidirectional.

illustrated in Fig. 14.

6.1.1. Dry sliding with steel vs steel surfaces

The friction and wear results obtained from the dry sliding steel vs steel experiments are similar to those reported in previous studies [16, 56]. The coefficients of friction, from 0.51 to 0.72, that we measured are typical values as well as the ball wear rates from 20 to 40 · 10^{-6} mm³/Nm and disc wear rates from 0.01 to 0.023 · 10^{-6} mm³/Nm.

In line with previous studies we observed the reduction in friction with higher surface roughness [5,56]. This can be explained by high adhesive force when smoother steel surfaces are in contact with each other. For rougher surfaces with ridges and valleys the sliding contact occurs at the contacting asperities, and thus is the real contact area that participates in the adhesive friction smaller, see Fig. 14.

No clear influence or trend was observed for the three topographic orientations. This is not surprising since the contact conditions in dry steel vs steel sliding are very severe. Thus, almost immediately after sliding begins the surface topography pattern is destroyed and a steel layer forms especially on the disc surfaces. The severity of the contact conditions is reflected by the high wear. This can be seen on the wear scar and wear track images in Fig. 6. It is interesting to compare our results with the findings of Rosenkranz et al. [42]. They observed topography orientation effects under much milder steel vs steel reciprocal linear sliding contacts with a load of 0.001 N and a speed of 0.001 m/s. They found lower friction for perpendicular 90° grooved topography compared to parallel 0° grooved topography. They measured a high friction coefficient of 1.2 for unpatterned steel surfaces but 0.5 for 0° parallel grooved and 0.4 for 90° perpendicular grooved surfaces.

An interesting novel feature, not previously observed or reported in the literature, was observed. In the experiments where the contact conditions were similar, we measured about 10% lower coefficient of friction in the ball-on-disc rotational experiments compared to those carried out with linear reciprocal sliding. The ball wear was in linear sliding of the same order of magnitude as in rotational sliding, and no difference could be observed in disc wear. This trend was the same for smooth, average and rough surfaces. This is perhaps due to the linear reciprocal sliding movement producing more commensurable grooves resulting in a larger real contact area and resulting in higher adhesive friction compared with the rotational movement where such grooves are not easily formed. Alternatively, maybe the reciprocal movement in linear sliding there is a surface texture destroying effect that is not seen in the same extent in continuous rotational sliding. Or alternatively, the higher static friction at the turning points could have some influence.
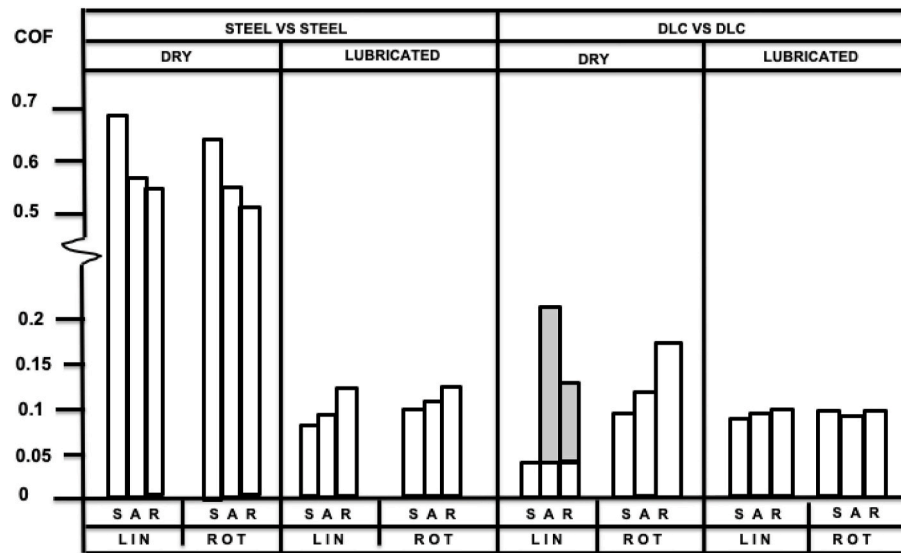
Fig. 4. Coefficients of friction (COF) in linear (LIN) and rotational (ROT) dry and lubricated sliding with smooth (S), average rough (A) and rough (R) steel vs steel and DLC vs DLC surfaces. The LIN columns represent average COF values of the three topographic orientations and when the difference was large the scatter is indicated by a grey column.
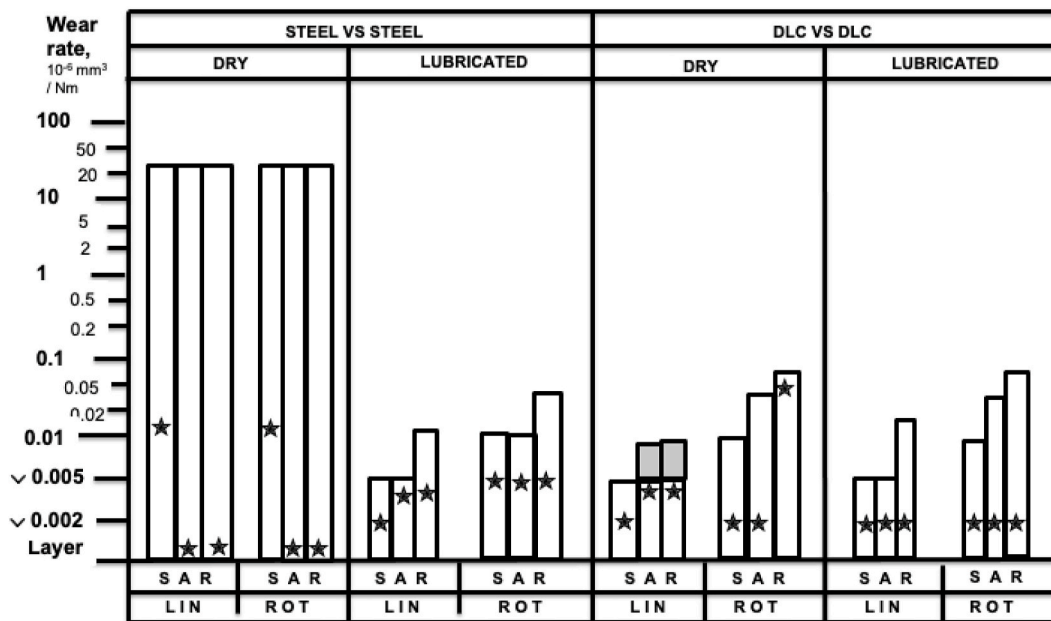

Fig. 5. Ball (column) and disc (star) wear rates in linear (LIN) and rotational (ROT) dry and lubricated sliding with smooth (S), average rough (A) and rough (R) steel vs steel and DLC vs DLC surfaces. The LIN columns represent average wear values of the three topographic orientations and when the difference was large the scatter is indicated by a grey column.

6.1.2. Lubricated sliding with steel vs steel surfaces

The lubricated sliding experiments with steel vs steel surfaces showed a similar friction and wear behavior to that what has been reported previously with coefficients of friction between 0.08 and 0.13 and with low wear rates below $0.04 \cdot 10^{-6}$ mm³/Nm [16,57,58]. Different from the dry contact experiments we now observed an increasing trend in the coefficient of friction with increasing surface roughness both in linear from 0.08 to 0.13 and in rotational sliding from 0.10 to 0.13. The experiments were carried out with low-speed sliding movement of only 0.01 m/s to prevent hydrodynamic effects. Thus, the lubrication mechanism in all experiments can be considered as boundary lubrication.

Under these conditions the adhesive friction was mainly prevented in lubricated sliding by a boundary lubrication film. The shearing of the film can much easily take place between smooth surfaces as compared to rough surfaces where the topography interferes with the shearing process and may cause some asperity collision effects. The typical structure, composition and properties of such synthetic oil boundary lubricant films have been described in the literature [6,8,65–67]. The PAO lubricant without boundary additives has relatively poor boundary lubrication properties as no surface chemical reactions are expected to take place at asperity vs asperity contacts [59].

The coefficient of friction as well as the measured wear were marginally higher in rotational sliding compared with linear sliding, but the difference is too small for any conclusions to be made. No topographic orientation effects could be observed in linear sliding. This
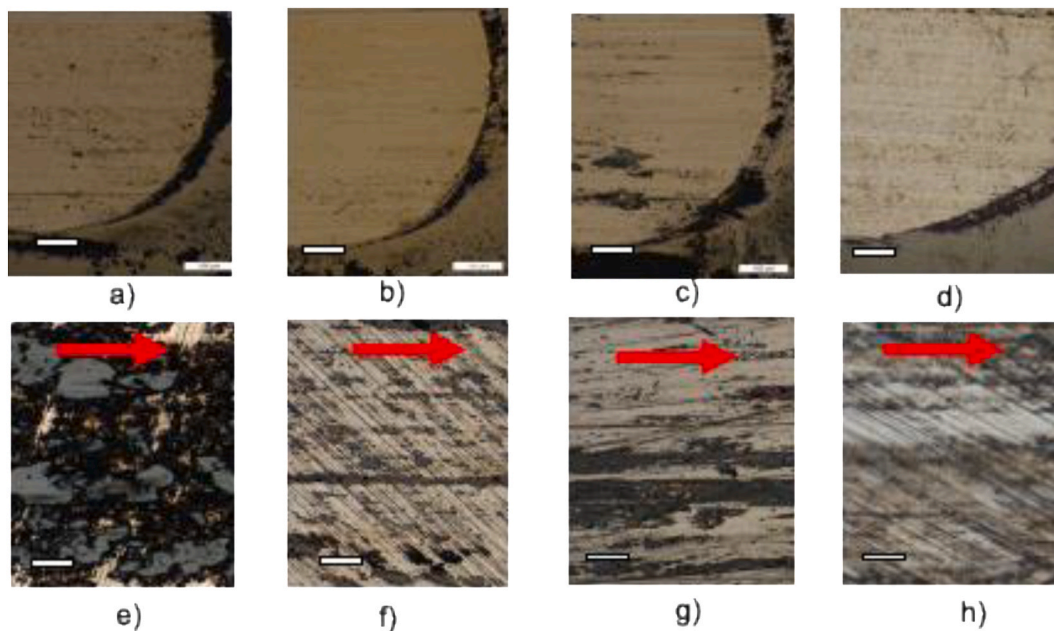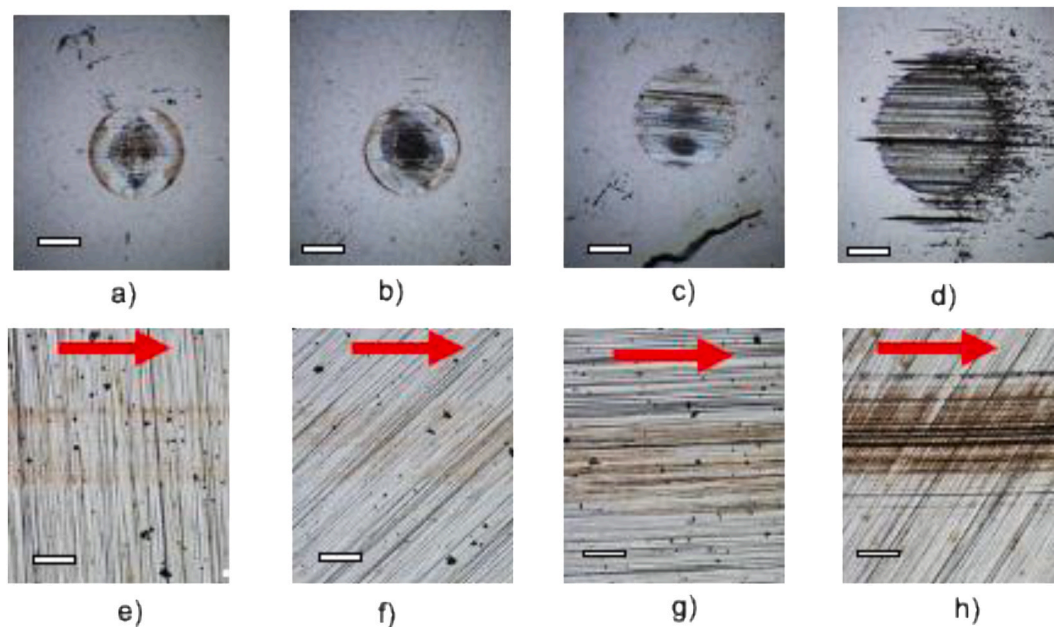
Fig. 6. Images of the wear scars of the balls and discs with average surface roughness after linear dry sliding of steel vs steel surfaces with 90° (a and e), 45° (b and f), and 0° (c and g) topographic orientation with regard to sliding direction and after rotational dry sliding (d and h). The red arrow indicates the sliding direction of the ball and the white bars show the scale of 100 μm. (For interpretation of the references to colour in this figure legend, the reader is referred to the Web version of this article.)

Fig. 7. Images of the wear scars of the balls and discs with average surface roughness after lubricated sliding of steel vs steel surfaces with 90° (a and e), 45° (b and f), and 0° (c and g) topography orientation with regard to sliding direction and after lubricated rotational sliding (d and h). The red arrows indicate the sliding direction of the while the white bars show the scale of 100 μm. (For interpretation of the references to colour in this figure legend, the reader is referred to the Web version of this article.)

indicates that the boundary lubrication film efficiently prevents steel to steel contacts between the sliding surfaces and offers a slippery layer for low shearing to take place both with smooth and rougher surfaces, see Figs. 7 and 14.

6.1.3. Dry sliding with DLC vs DLC surfaces

Extremely low friction with a coefficient 0.04 was measured in linear dry sliding for smooth DLC vs DLC surfaces. The low level of friction was also observed for average rough and rough surfaces with 0° topographic orientation. This extremely low level of friction has previously been reported by other investigators [15,16,18,58,60,61,71,73] and it can be attributed to the formation of a graphitic super-lubricious and stable thin DLC surface layer on the asperity tips. It is well known that the dry friction of DLC coated surfaces can be very low, and several explanations related to H termination of the DLC surface have been published. The typical structure, composition and properties of such super-lubricious
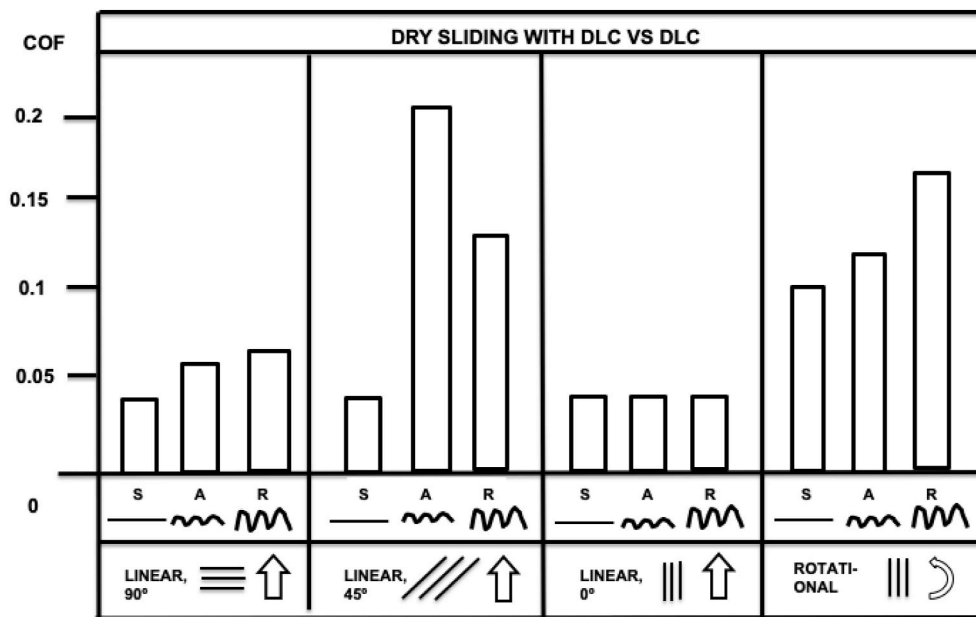
Fig. 8. Coefficients of friction (COF) in linear and rotational dry sliding with smooth (S), average rough (A) and rough (R) DLC vs DLC surfaces and with four topographic orientations.
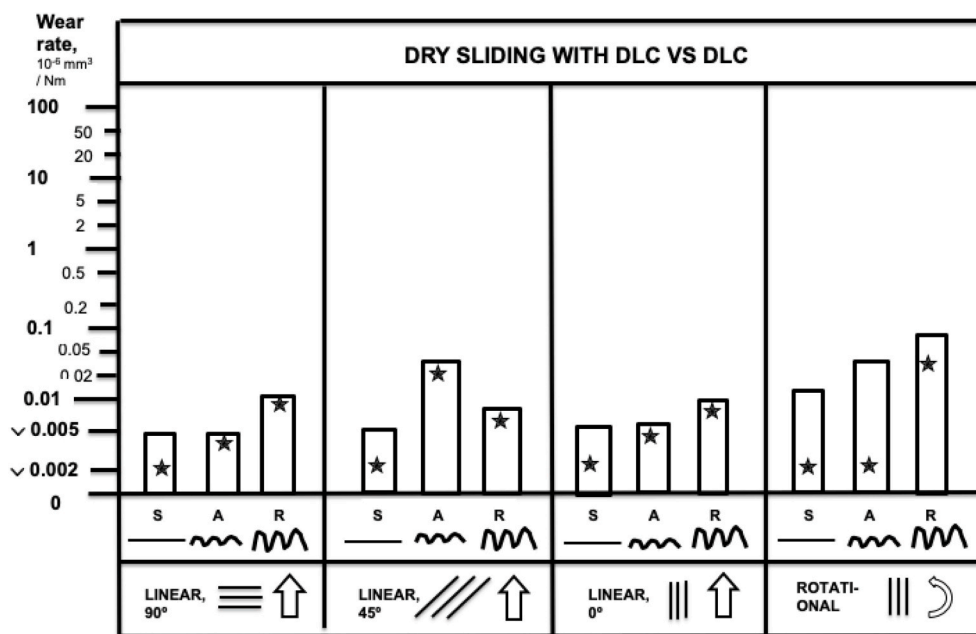

Fig. 9. Ball (column) and disc (star) wear rates in linear and rotational dry sliding with smooth (S), average rough(A) and rough (R) DLC vs DLC surfaces and with four topographic orientations.

DLC surface layers formed on steel surfaces have been described in the literature [8,68–71,73].

The slippery super-lubricious layer formation process seems to be interrupted by topographic effects especially at 45° orientation during linear sliding with average rough surfaces and to some extent also by 90° and 45° orientations with rough surfaces as well as in rotational sliding, as can be seen in Fig. 8. Corresponding effects could also be observed in the wear results, see Fig. 9, but here the uncertainty is much higher because of the extremely low values of wear measured.

An interesting result is that the most severe topographic disturbance on the layer formation accompanied by the highest coefficient of friction was during linear sliding with average roughness and 45° topographic orientation. Then the coefficient of friction increased about five times to a value of 0.21. The remarkable difference in contact mechanics, when sliding with 0° and 45° topographic orientation, is also clearly reflected in the ball wear scars morphology as shown in Fig. 10 b and c. This behavior can probably be explained by the contact dynamics in the situation where both the ball and the disc surfaces have about the same surface roughness R_a of 0.010 and 0.012 μm. Thus, the commensurate surfaces interlock strongly into each other and the 45° orientation results in strong disruptions to the film formation and strong side forces when sliding and subsequent high friction. It is worth noticing that for the average rough surface, the FS_0 and FS_{45} were 2.55 and 2.65 respectively, which may indicate that the higher FS in the direction of
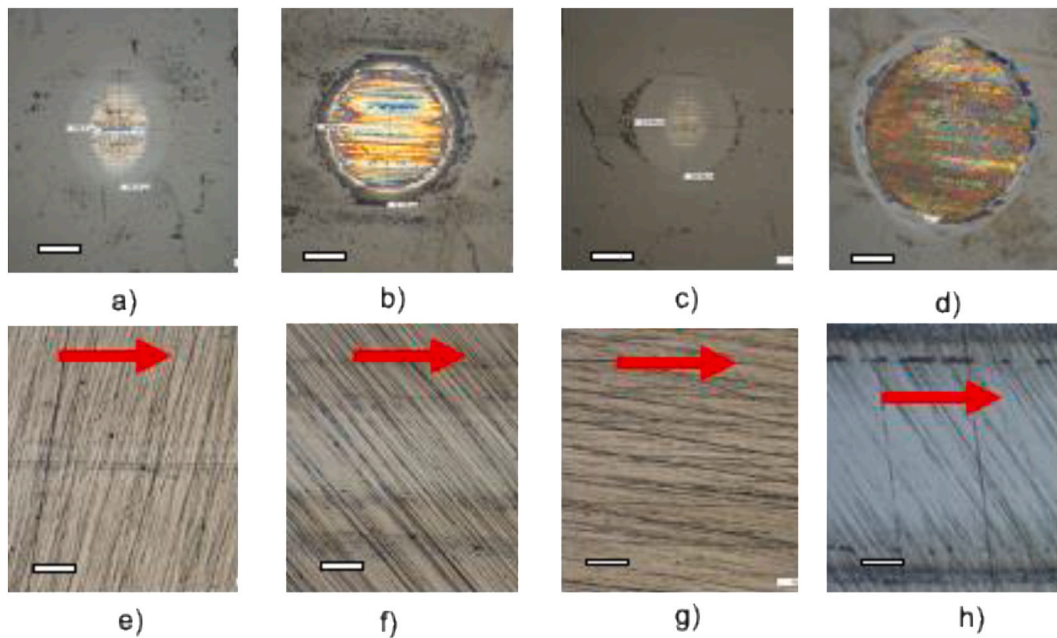
Fig. 10. Images of the wear scars of the balls and average rough discs after linear dry sliding of DLC vs DLC surfaces with 90° (a and e), 45° (b and f), and 0° (c and g) topographic orientation with regard to sliding direction and after rotational dry sliding (d and h). The red arrows indicate the sliding direction of the ball while the white bars show the scale of 100 μm. (For interpretation of the references to colour in this figure legend, the reader is referred to the Web version of this article.)
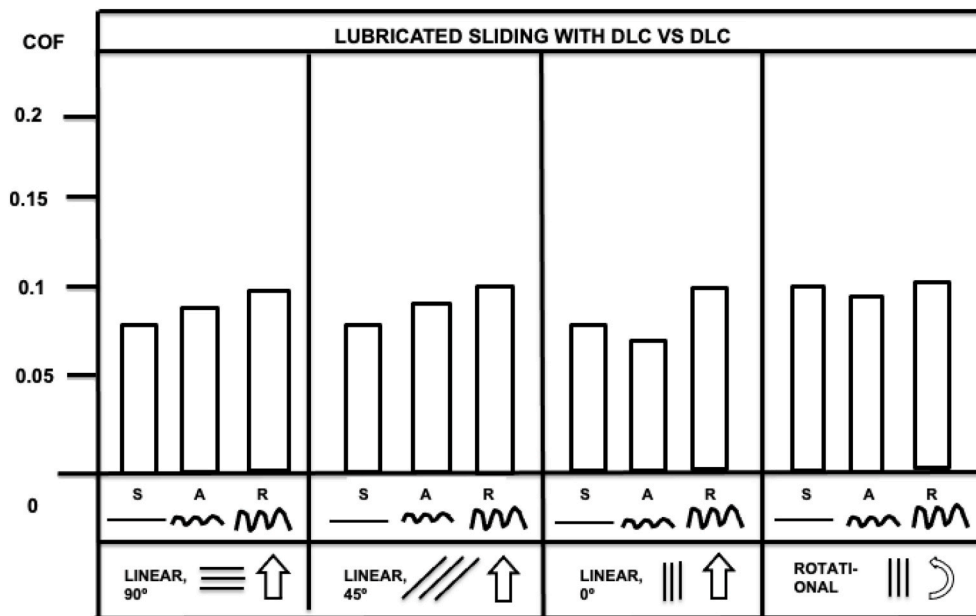
Fig. 11. Coefficients of friction (COF) in linear and rotational lubricated sliding with smooth (S), average rough (A) and rough (R) DLC vs DLC surfaces and with four topographic orientations.

45°, as compared to 0°, reflects on the increased friction observed. The coating was worn out with 90° and 45° topographic orientation as seen in Fig. 10.

There was an increase in both friction, from 0.10 to 0.17, and in wear, from 0.01 to 0.08 · 10^{-6} mm^3/Nm, with increased surface roughness in rotational sliding. The same trend of increased friction and wear of the same magnitude, with increasing surface roughness in BOD testing with tungsten and chromium doped DLC coatings has been reported by Svanh et al. [18] and for non-doped DLC by Jiang and Arnell [17].

It is also interesting to note that the super-lubricious film is fully formed and works well with smooth as well as rougher surfaces when the topography orientation is same as the direction of sliding as is in the case of 0° topographic orientation. The surface layer formation is to some extent disturbed when the topography orientation is perpendicular to sliding direction, as it is with 90° orientation, and most disturbed with 45° orientation. The uninterrupted and continuous sliding on the counter surface, as it takes place both with smooth surfaces and along the topography ridges in 0° orientation, seems to offer good and stable conditions for the super-lubricious layer to be produced.

Considerably higher values of the coefficient of friction were measured during rotational sliding compared with the ideal low friction
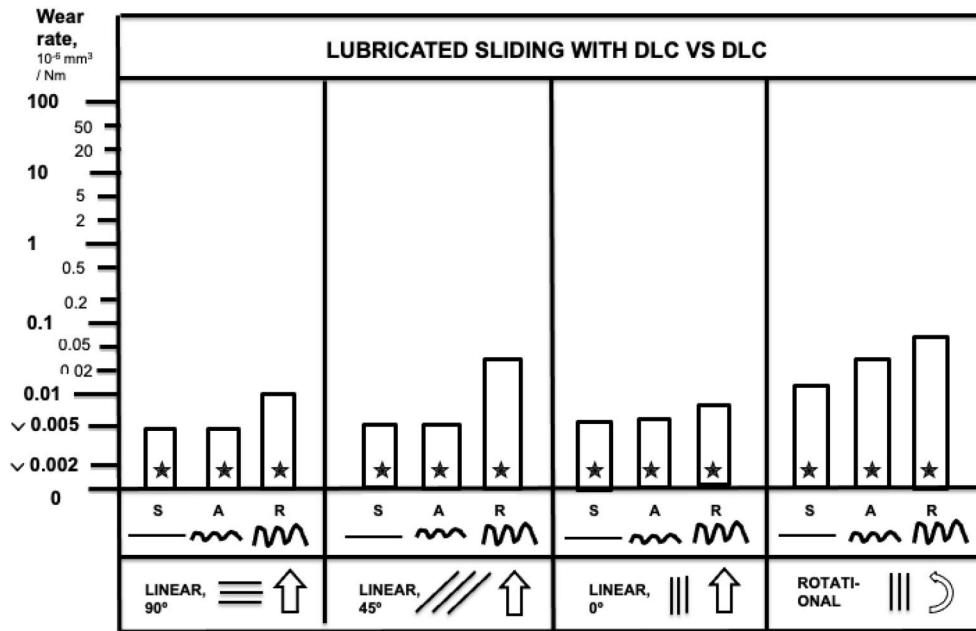
Fig. 12. Ball (column) and disc (star) wear rates in linear and rotational lubricated sliding with smooth (S), average rough (A) and rough (R) DLC vs DLC surfaces and with four topographic orientations.
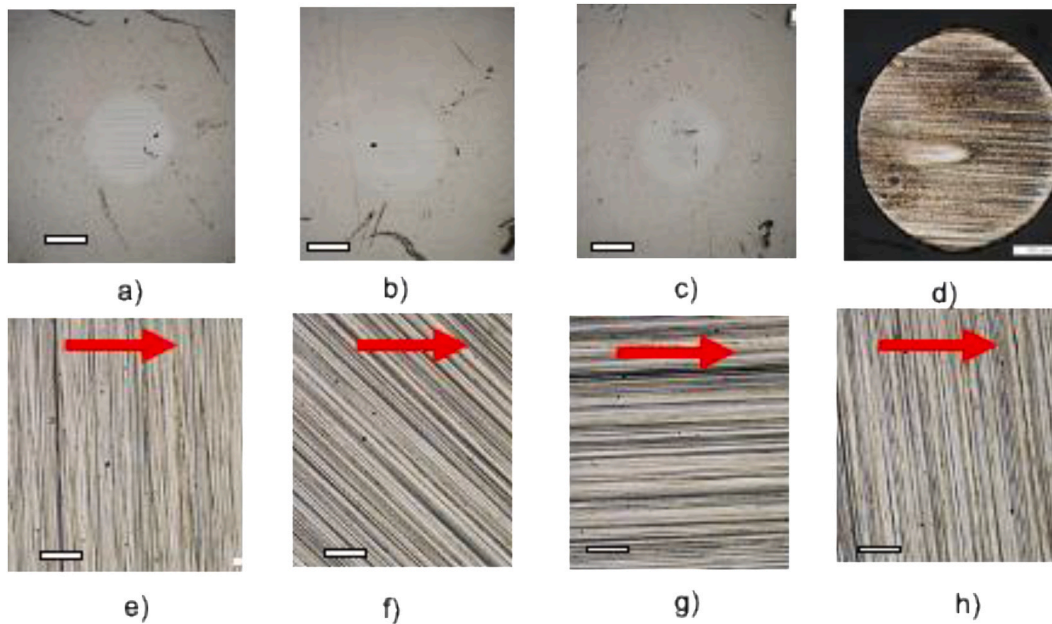

Fig. 13. Images of the wear scars of the ball and average rough discs after lubricated sliding of DLC vs DLC surfaces with 90° (a and e), 45° (b and f), and 0° (c and g) topographic orientation with regard to sliding direction and after rotational lubricated sliding (d and h). The red arrows show the sliding direction of the ball while the white bars show the scale of 100 μm. (For interpretation of the references to colour in this figure legend, the reader is referred to the Web version of this article.)

in linear sliding indicating that the rotational movement is also disturbing and represents no ideal condition for the formation of the super-lubricious surface layer.

6.1.4. Lubricated sliding with DLC vs DLC surfaces

The friction and wear results, i.e., coefficient of friction between 0.07 and 0.10 and wear rate below $0.08 \cdot 10^{-6}$ mm^3/Nm in lubricated sliding with DLC vs DLC surfaces, are similar to those measured with steel vs steel lubricated surfaces under the same conditions. This indicates that oil lubrication affects the contact conditions as reported earlier [63,72, 73]. A proper boundary lubricant film, as described in § 6.1.2, is formed

on the asperity tops of the DLC coated surfaces and the shearing takes place within this layer without influence of the DLC layer below, as illustrated in Figs. 13 and 14. The lubricant film prevents the super-lubricious DLC layer to be formed. Similar observations under the same contact conditions, where friction is about three times higher in oil lubricated DLC vs DLC contacts compared to dry contacts, have been reported by Velkavrh and Kalin [16]. However, Abdullah Tasdemir et al. [58] report very low friction coefficients, between 0.02 and 0.04, for PAO base oil and three PAO + additive packages with ta-C DLC vs ta-C DLC coated surfaces at a higher speed of 0.1 m/s and a lower load of 5 N. Miyake et al. [59] have shown that PAO itself is not lubricating well DLC
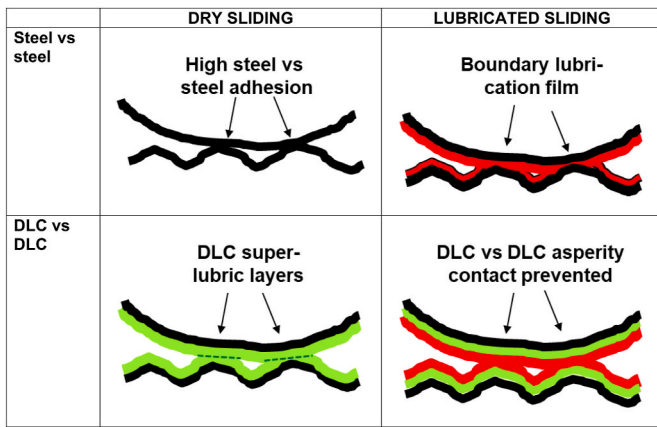
Fig. 14. Illustrations of the sliding contact mechanisms observed with steel and DLC surfaces.

coated surfaces but additives, such as esters, can reduce friction compared to pure PAO in lubricated contacts.

It is interesting to note that the coefficient of friction was of almost at the same level in all cases investigated while an increase in ball wear with surface roughness was observed, as seen in Figs. 4 and 5. The disc wear was all the time very low and hardly detectable. This discrepancy is explained by the contact conditions, i.e., move from smooth lubricated DLC vs DLC sliding into a harsher transition region where increasing disc surface roughness interrupts the smooth sliding. The disturbance in the contact is interestingly first observed as increased ball wear, i.e., when the point contact pressure is very high. At this early stage of transition, the friction and disc wear are still on an unchanged level. The changes in contact conditions are then reflected in the wear scar and wear track, as shown in Fig. 13.

6.2. Comparison with others results

We found in literature three studies where friction and wear measurements had been carried out with materials and in conditions comparable to ours [16,42,58]. The key parameters used by these investigators and in our study are presented in Table 2.

By comparing the results from these four investigations we can make the following observations:

- No topographic orientation effects could be observed in the tests of the present investigation due to the severe contact conditions that quickly destroyed the topography profiles. Rosenkranz et al. [42] found topographic effects under much milder contact conditions with extremely low load and sliding speed. They found that a perpendicular 90° grooved topography resulted in less friction than a parallel 0° grooved topography.

- Both Velkavrh and Kalin [16] and our present investigation found super-lubricious very low friction in dry DLC sliding (0.04) while friction was about two to three times higher (0.08–0.12) when PAO oil was introduced.

- Abdullah et al. [58] measured ultralow friction with a coefficient of about 0.02 for PAO lubricated and 0.02–0.04 for PAO with additive (glycerol mono-oleate and/or ZnDTP) lubricated sliding. This discrepancy is not clear but may be due to the sliding conditions. Abdullah et al. used with much higher speed, lower load and a cylindrical pin surface, which can easily create hydrodynamic effects at higher velocities. A problem with Abdullah's et al. work is that they do not report any results for dry DLC sliding for comparison.

6.3. Experimental uncertainty

The analysis and the subsequent conclusions are mainly based on the measured friction results. The wear results are used as complementary information because of the uncertainty that arises from the uncontrolled nature of wear process and the very low wear values measured. In some cases, wear was even below what was possible to detect. The experimental repeatability was good as can be seen in Tables A1 and A2 in Appendix 1.

The results obtained for dry linear sliding with DLC vs DLC coated surfaces were double checked against the results reported earlier by Holmberg et al. [50]. It was noted that the reported ball wear results were two orders of magnitude higher compared with what they were in reality. This error has been corrected in the present work.

The comparison of our results with those obtained by Velkavrh and Kalin [16] with steel vs steel and DLC vs DLC contacts under similar conditions shows a very good agreement. However, their study was limited in scope since the they did not investigate the influence of surface roughness and topography, as they carried out all their experiments with only one roughness combination of R_a value 0.05 μm for the steel disc and 0.03 μm for the spherical steel pin.

7. Conclusions

Tribological experiments were carried out with smooth, average rough and rough (in range of 0.004–0.11 R_a values and FSs in range from 2.21 to 2.94) steel and DLC coated surfaces under dry and synthetic PAO oil lubricated conditions. The grooved topography surface pattern orientation with regard to sliding direction was 0°, 45° and 90° in linear reciprocal sliding and 0–360° in continuous rotational sliding. The load was 20 N and the sliding speed 0.1 m/s. Based on friction and wear measurements and wear scar observations the following conclusions can be drawn:

1. **In dry sliding steel vs steel contacts**, the coefficient of friction decreased with increasing surface roughness from values of about 0.67 down to 0.53. The decrease in friction with higher surface

Table 2

Key tribo-parameters and observations in four investigations on topography effects on friction and wear.

Investigators reference	Load (N) & speed (m/s)	Sliding movement	Lubrication	Materials	Roughness, Ra (μm)	Observations
Holmberg et al.[a]	20 & 0.01	- linear reciprocal - rotational	- dry - PAO	- steel - DLC a-C	0.004–0.11 grooved	- no orientational effects in steel vs steel - dry DLC μ < oil DLC μ - ultralow friction only for dry DLC
Velkavrh & Kalin [16]	10 & 0.003–0.04	- linear reciprocal	- dry - PAO	- steel - DLC a-CH	0.03–0.05	- dry DLC μ < oil DLC μ - ultralow friction only for dry DLC
Rosenkranz et al. [42]	0.001 & 0.001	- linear reciprocal	- dry	- steel	0.35 grooved	- orientational effects in steel vs steel, μ 90° < μ 0°
Abdullah et al. [58]	5 & 0.1	- rotational	- PAO - PAO + additives	- DLC ta-C	0.003–0.25	- ultralow friction for dry and PAO lubricated DLC - no results from dry DLC

[a] = present investigation; μ = coefficient of friction.

roughness is due to lower adhesive friction in contacts with rougher surfaces as the load is carried to a larger extent by the asperity tips. The topography orientation had almost no effect as the topographic pattern was largely destroyed by the wear process. Topography orientation effects in steel vs steel contacts have been observed at considerably lower load and speed conditions by others [42].

2. **In oil lubricated steel vs steel contacts**, the coefficient of friction, on the other hand, increased with surface roughness from values of 0.08–0.13. The oil prevents efficiently the adhesive friction between the surfaces. The increase in friction for rougher surfaces is explained by the effect of the lubricant film shearing, which is easier between smooth than with rougher surfaces. This results in disturbances in the shear plane and the shearing process. The topographic orientation had almost no effect as the film exhibited good load carrying capacity allowing for the shearing to take place in the lubricant film on asperity tips regardless of the topographic pattern.

3. **In dry sliding DLC vs DLC contacts,** there was a considerable effect of surface roughness and topographic orientation on friction and wear. A super-lubricious DLC surface layer was efficiently formed in the contact and resulted in very low coefficients of friction of 0.04 with smooth and rough surfaces when the surface topographic direction was the same as the sliding direction. However, the surface layer formation was most severely disturbed and resulted in a coefficient of friction five times higher of 0.21 with 45° topographic orientation and surfaces with same level of roughness on both sides in the contact. This resulted in strong surface topographic interlocking combined with strong side directional disturbing forces. The super-lubricious layer formation was also disturbed by the rotational sliding direction resulting in high friction coefficients of 0.10–0.17.

4. **In oil lubricated DLC vs DLC contacts,** the oil prevented the formation of the super-lubricious surface layer both in linear and rotational sliding. It resulted in contact conditions where the shearing took place in the boundary lubricant film without the influence from the DLC layers. This is similar to the tribological contact mechanism observed in lubricated uncoated steel vs steel contacts. A slight increase in friction and wear could be observed in lubricated DLC contacts, however, only minor topographic orientation effects were observed.

5. **Impact of sliding direction.** In continuous rotational sliding the coefficient of friction was 10% lower compared to linear reciprocating sliding with dry steel vs steel surfaces for all three roughness

levels. This may be due to the differences in the formation of commensurable wear grooves or in variations in the surface texture destroying effects. The favorable super-lubricious low friction DLC vs DLC sliding conditions with a coefficient of friction of 0.04 appeared only during linear sliding. In rotational sliding, the coefficient of friction was between two up to two and a half times higher.

Declaration of competing interest

Appendix

Table A1
Friction in lubricated linear reciprocating ball-on-plate and rotational ball-on-disc testing.

Coefficient of friction in linear reciprocating pin-on-plate and rotational pin-disc testing		Linear reciprocating pin-on-plate test									Rotational pin-on-disc test
Surface material	Orientation	1st cycle, 1 N	2nd cycle, 1 N	3rd cycle, 1 N	4th cycle, 1 N	5th cycle, 1 N	10th cycle, 1 N	100th cycle, 3 N	30 min, 20 N	Stable friction, 20 N	Stable friction, 20 N
DLC smooth	0 degrees	0.08±0.04	0.06±0.02	0.05±0.02	0.05±0.02	0.05±0.02	0.05±0.02	0.08±0.01	0.07±0.02	0.08±0.02	
	45 degrees	0.06±0.03	0.06±0.02	0.05±0.02	0.05±0.02	0.05±0.02	0.05±0.02	0.08±0.01	0.08±0.03	0.08±0.02	0.10±0.02 *
	90 degrees	0.07±0.03	0.06±0.02	0.05±0.02	0.05±0.02	0.05±0.02	0.05±0.02	0.08±0.01	0.07±0.03	0.08±0.02	
DLC average	0 degrees	0.08±0.02	0.07±0.02	0.07±0.02	0.07±0.02	0.06±0.02	0.06±0.02	0.08±0.01	0.07±0.03	0.07±0.02	
	45 degrees	0.09±0.02	0.08±0.02	0.08±0.02	0.08±0.02	0.08±0.02	0.07±0.02	0.09±0.01	0.08±0.03	0.09±0.02	0.09±0.02 *
	90 degrees	0.09±0.02	0.09±0.03	0.08±0.02	0.08±0.02	0.08±0.02	0.08±0.02	0.09±0.01	0.08±0.03	0.09±0.02	
DLC rough	0 degrees	0.12±0.04	0.12±0.05	0.12±0.05	0.12±0.05	0.12±0.05	0.10±0.04	0.11±0.02	0.10±0.03	0.10±0.02 *	
	45 degrees	0.11±0.03	0.10±0.03	0.09±0.03	0.09±0.03	0.09±0.03	0.09±0.03	0.10±0.02	0.10±0.03	0.10±0.02 *	0.10±0.01 *
	90 degrees	0.10±0.03	0.10±0.03	0.09±0.03	0.09±0.03	0.09±0.03	0.09±0.03	0.09±0.03	0.09±0.03	0.10±0.02 *	
steel smooth	0 degrees	0.06±0.03	0.06±0.03	0.06±0.03	0.06±0.02	0.07±0.03	0.07±0.03	0.08±0.01	0.08±0.03	0.08±0.02	
	45 degrees	0.05±0.02	0.05±0.02	0.05±0.01	0.05±0.01	0.05±0.02	0.05±0.02	0.08±0.01	0.08±0.03	0.08±0.02	0.10±0.01
	90 degrees	0.06±0.03	0.07±0.03	0.06±0.03	0.06±0.03	0.06±0.03	0.06±0.03	0.08±0.01	0.07±0.03	0.08±0.02	
steel average	0 degrees	0.12±0.04	0.12±0.05	0.12±0.05	0.12±0.06	0.12±0.06	0.10±0.04	0.11±0.02	0.10±0.03	0.10±0.02	
	45 degrees	0.08±0.03	0.08±0.03	0.08±0.03	0.08±0.03	0.08±0.03	0.08±0.03	0.09±0.01	0.08±0.03	0.09±0.02	0.11±0.01
	90 degrees	0.08±0.02	0.08±0.03	0.08±0.02	0.08±0.02	0.08±0.03	0.08±0.03	0.09±0.01	0.08±0.03	0.09±0.02	
steel rough	0 degrees	0.27±0.08	0.29±0.07	0.30±0.08	0.31±0.09	0.31±0.09	0.30±0.09	0.24±0.05	0.12±0.05	0.13±0.03	
	45 degrees	0.14±0.03	0.14±0.02	0.14±0.03	0.14±0.03	0.14±0.03	0.14±0.03	0.14±0.03	0.12±0.04	0.13±0.03	0.13±0.02
	90 degrees	0.14±0.04	0.13±0.03	0.13±0.03	0.13±0.03	0.13±0.03	0.13±0.03	0.13±0.03	0.12±0.09	0.13±0.07	

* = coating on ball worn through in two or more tests

* = coating on ball worn out in two or more test

Table A2

Friction and wear in lubricated linear reciprocating ball-on-plate and rotational ball-on-disc testing.

Performance	Symbol (unit)	DLC-S vs DLC-B	DLC-A vs DLC-B	DLC-R vs DLC-B	STE-S vs STE-B	STE-A vs STE-B	STE-R vs STE-B
Linear reciprocal ball-on-plate test							
1. Friction in PoP at 0°	μ (dimensionless)	**0.08±0.02**	**0.07±0.02**	**0.10±0.02**	**0.08±0.02**	**0.09±0.02**	**0.13±0.03**
2. Wear rate in PoP at 0°	K_{pin} (10^{-6} mm^3/Nm) /K_{disk} (10^{-6} mm^3/Nm)	**<0.005 /<0.002**	**<0.005 /<0.002**	**<0.005 /<0.002**	**<0.005 /<0.002**	**0.005±0.003 /<0.002**	**0.010±0.003 /<0.002**
3. Friction in PoP at 45°	μ (dimensionless)	**0.08±0.02**	**0.09±0.02**	**0.10±0.02**	**0.08±0.02**	**0.09±0.02**	**0.13±0.03**
4. Wear rate in PoP at 45°	K_{pin} (10^{-6} mm^3/Nm) /K_{disk} (10^{-6} mm^3/Nm)	**<0.005 /<0.002**	**<0.005 /<0.002**	**0.030±0.010 /<0.002**	**<0.005 /<0.002**	**0.005±0.0030 /<0.005**	**0.010±0.003 /<0.005**
5. Friction in PoP at 90°	μ (dimensionless)	**0.08±0.02**	**0.09±0.02**	**0.10±0.02**	**0.08±0.02**	**0.09±0.02**	**0.13±0.03**
6. Wear rate in PoP at 90°	K_{pin} (10^{-6} mm^3/Nm) /K_{disk} (10^{-6} mm^3/Nm)	**<0.005 /<0.002**	**<0.005 /<0.002**	**0.010±0.003 /<0.002**	**<0.005 /<0.002**	**0.005±0.003 /<0.005**	**0.010±0.003 /<0.005**
Rotational ball-on-disc test							
7. Friction in PoD	μ (dimensionless)	**0.10±0.02**	**0.09±0.02**	**0.10±0.01**	**0.10±0.01**	**0.11±0.01**	**0.13±0.02**
8. Wear rate in PoD	K_{pin} (10^{-6} mm^3/Nm) /K_{disk} (10^{-6} mm^3/Nm)	**0.010±0.003 /<0.002**	**0.040±0.006 /<0.002**	**0.080±0.010 /<0.002**	**0.010±0.006 /<0.005**	**0.010±0.006 /<0.005**	**0.040±0.006 /<0.005**

NW = No wear observed (<0.002 · 10^{-6} mm^3/Nm); MW = mild wear observed (0.002–0.005 · 10^{-6} mm^3/Nm).

References

[1] K. Holmberg, P. Andersson, A. Erdemir, Global energy consumption due to friction in passenger cars, Tribol. Int. 47 (2012) 221–234.

[2] K. Holmberg, P. Kivikytö-Reponen, P. Härkisaari, K. Valtonen, A. Erdemir, Global energy consumption due to friction and wear in the mining industry, Tribol. Int. 115 (2017) 116–139.

[3] K. Holmberg, A. Erdemir, Influence of tribology on global energy consumption, costs and emissions, Friction 5 (2017) 236–284.

[4] K. Holmberg, A. Erdemir, The impact of tribology on energy use and CO$_2$ emission globally and in combustion engine and electric cars, Tribol. Int. 135 (2019) 389–396.

[5] F.P. Bowden, D. Tabor, Friction and Lubrication of Solids, Part II, Oxford University Press, Oxford, UK, 1964.

[6] G. Stachowiak, G.W. Batchelor, Engineering Tribology, Amsterdam, The Netherlands, fourth ed., 2013.

[7] I. Hutchings, P. Shipway, Tribology – Friction and Wear of Engineering Materials, second ed., Butterworth-Heinemann, Oxford, UK, 2017.

[8] K. Holmberg, A. Matthews, Coatings Tribology: Properties, Mechanisms, Techniques and Applications in Surface Engineering, in: Elsevier Tribology and Interface Engineering Series No. 56, Elsevier, Amsterdam, The Netherlands, 2009.

[9] J. Halling, A contribution to the theory of mechanical wear, Wear 34 (1975) 239–249.

[10] J. Halling, Toward a mechanical wear equation, Journal of Lubrication Technology, Trans. ASME 105 (1983) 212–219.

[11] M. El-Sherbiny, J. Halling, The role of surface roughness in the friction of sliding contacts, Tribol. Int. 17 (1984) 223–227.

[12] N. Patir, H.S. Cheng, An average flow model for determining effects of three-dimensional roughness on partial hydrodynamic lubrication, Transactions of ASME, Journal of Lubrication Technology100 (1978) 12–17.

[13] J. Keller, V. Fridrici, P. Kapsa, J.F. Huard, Surface topography and tribology of cast iron in boundary lubrication, Tribol. Int. 42 (2009) 1011–1018.

[14] M. Kalin, I. Velkavrh, J. Vizintin, L. Ozbolt, Review of boundary lubrication mechanisms of DLC coatings used in mechanical applications, Meccanica 43 (2008) 623–637.

[15] K. Topolovec-Miklozic, F. Lockwood, H. Spikes, Behaviour of boundary lubricating additives on DLC coatings, Wear 265 (2008) 1893–1901.

[16] I. Velkavrh, M. Kalin, Effect of base oil lubrication in comparison with non-lubricated sliding in diamond-like carbon contacts, Tribology 5 (2011) 53–58.

[17] J. Jiang, R.D. Arnell, The effect of substrate surface roughness on wear of DLC coatings, Wear 239 (2000) 1–9.

[18] F. Svahn, Å. Kassman-Rudolphi, E. Wallen, The influence of surface roughness on friction and wear of machine element coatings, Wear 254 (2003) 1092–1098.

[19] V. Westerlund, J. Heinrichs, M. Olsson, S. Jacobson, Investigation of material transfer in sliding friction-topography or surface chemistry? Tribol. Int. 100 (2016) 213–223.

[20] M. Masuko, T. Kudo, A. Suzuki, Effect of surface roughening of substrate steel on the improvement of delamination strength and tribological behavior of hydrogen amorphous carbon coating under lubricated conditions, Tribol. Lett. 51 (2013) 181–190.

[21] K. Holmberg, Friction in Low-Speed Lubricated Rolling and Sliding Contacts, PhD Thesis, Helsinki University of Technology, VTT Publications 16/1984. Espoo, VTT. 81 p.

[22] A. Al-Azizi, O. Eryilmaz, A. Erdemir, S.H. Kim, Effects of nanoscale surface texture and lubricant molecular structure on boundary lubrication in liquid, Langmuir 29 (2013) 13419–13426.

[23] C. Gachot, A. Rosenkranz, S.M. Hsu, H.L. Costa, A critical asset of surface texturing for friction and wear improvement, Wear 372–373 (2017) 21–41.

[24] I. Etsion, Modeling of surface texturing in hydrodynamic lubrication, Friction 1 (2013) 195–209.

[25] L. Wang, Use of structured surfaces for friction and wear control on bearing surfaces, Surf. Topogr. Metrol. Prop. 2 (2014) 1–9.

[26] I. Etsion, E. Sher, Improving fuel efficiency with laser surface textured piston rings, Tribol. Int. 42 (2009) 542–547.

[27] A. Ramesh, W. Akram, S.P. Mishra, A.H. Cannon, A.A. Polycarpou, W.P. King, Friction characteristics of microtextured surfaces under mixed and hydrodynamic lubrication, Tribol. Int. 57 (2013) 170–176.

[28] R.D. Britton, C.D. Elcoate, M.P. Alanou, H.P. Evans, R.W. Snidle, Effect of surface finish on gear tooth friction, Transactions of the ASME, J. Tribol. 122 (2000) 354–360.

[29] Y. Ishida, H. Usami, Y. Hoshino, Effect of micro dimples on frictional properties in boundary lubrication condition, Kyoto, Japan, in: Proceedings of the World Tribology Congress, 9, 2009, pp. 6–11.

[30] W. Koszela, P. Pawlus, R. Reizer, T. Liskiewicz, The combined effect of surface texturing and DLC coating on the functional properties of internal combustion engines, Tribol. Int. 127 (2018) 470–477.

[31] H. Liu, H. Liu, C. Zhu, P. Wei, J. Tang, Tribological behavior of coated spur gear pairs with tooth surface roughness, Friction 7 (2019) 117–128.

[32] E.J. Abbott, F.A. Firestone, Specifying surface quality – a method based on accurate measurement and comparison, Mechanical Engineering (1933) 569–572. September.

[33] J.A. Greenwood, J.B.P. Williamson, Contact of nominally flat surfaces, Proceedings of the Royal Society in London A, Mathematical, Physical and Engineering Sciences 295 (1966) 300–319.

[34] W.K. Kubin, M. Pletz, W. Daves, S. Scheriau, A new roughness parameter to evaluate the near-surface deformation in dry rolling/sliding contact, Tribol. Int. 67 (2013) 132–139.

[35] G.E. Moales-Espejel, A. Gabelli, A major step forward in life modelling – the SKF generalized bearing life model – the power of tribology, Evolution – Business and Technology from SKF 4 (2015) 21–28.

[36] M. Kalin, A. Pogacnik, I. Etsion, B. Raeymaekers, Comparing surface topography parameters of rough surfaces obtained with spectral moments and deterministic methods, Tribol. Int. 93 (2016) 137–141.

[37] M. Wolski, P. Podsiadlo, G.W. Stachowiak, Applications of the variance orientation transform method to the multi-scale characterization of surface roughness and anisotropy, Tribol. Int. 43 (2010) 2203–2215.

[38] M. Wolski, P. Podsiadlo, G.W. Stachowiak, Directional fractal signature analysis of self-structured surface textures, Tribol. Lett. 47 (3) (2012) 323–340.

[39] M. Wolski, P. Podsiadlo, G.W. Stachowiak, K. Holmberg, A. Laukkanen, H. Ronkainen, M. Gee, J. Nunn, C. Gachot, L. Li, Multiscale characterization of 3D surface topography of DLC coated and uncoated surfaces by directional blanket covering (DBC) method, Wear 388–389 (2017) 47–56.

[40] D. Zhu, Y. Hu, Effects of rough surface topography and orientation on the characteristics of EHD and mixed lubrication in both circular and elliptical contacts, Tribol. Trans. 44 (2001) 391–398.

[41] B. Podgornik, J. Jerina, Surface topography effect on galling resistance of coated and uncoated tool steel, Surf. Coating. Technol. 206 (2012) 2792–2800.

[42] A. Rosenkranz, L. Reinert, C. Gachot, F. Mücklich, Alignment and wear debris effects between laser-patterned steel surfaces under dry sliding conditions, Wear 318 (2014) 49–61.

[43] M. Kalin, A. Pogacnik, Criteria and properties of the asperity peaks on 3D engineering surfaces, Wear 308 (2013) 95–104.

[44] S. Kucharski, G. Starzynski, Study of contact of rough surfaces: modeling and experiment, Wear 311 (2014) 167–179.

[45] S. Reichert, B. Lorentz, S. Heldmaier, A. Albers, Wear simulation in non-lubricated and mixed lubricated contacts taking into account the microscale roughness, Tribol. Int. 100 (2016) 272–279.

[46] X. Zheng, H. Zhu, A. Kiet Tieu, B. Kosasih, A molecular dynamics simulation of 3D rough lubricated contact, Tribol. Int. 67 (2013) 217–221.

[47] C. Gachot, A. Rosenkranz, L. Reinert, E. Ramos-Moore, N. Souza, M.H. Müser, F. Mucklich, Dry friction between laser-patterned surfaces: role of alignment, structural wavelength and surface chemistry, Tribol. Lett. 49 (2013) 193–202.

[48] N. Prodanov, C. Gachot, A. Rosenkranz, F. Mücklich, M.H. Muser, Contact mechanics of laser-textured surfaces – correlating contact area and friction, Tribol. Lett. 50 (2013) 41–48.

[49] Y. Xiao, W. Shi, Z. Han, J. Luo, L. Xu, Residual stress and its effect on failure in a DLC coating on a steel substrate with rough surfaces, Diam. Relat. Mater. 66 (2016) 23–35.

[50] K. Holmberg, A. Laukkanen, H. Ronkainen, R. Waudby, G. Stachowiak, M. Wolski, P. Podsiadlo, M. Gee, J. Nunn, C. Gachot, L. Li, Topographical orientation effects on friction and wear in sliding DLC and steel contacts, Part 1: Experimental, Wear 330–331 (2015) 3–22.

[51] M. Gee, J. Nunn, K. Holmberg, L. Li, G. Stachowiak, C. Gachot, Surface roughness effects on cumulative sliding wear of DLC and steel surfaces (Toronto, Canada), 20th International Conference on Wear of Materials 4 (2015) 12–16.

[52] K. Holmberg, A. Laukkanen, Wear models, in: second ed., in: R. Bruce (Ed.), Handbook on Lubrication and Tribology, Vol II Theory and Design, 13, CRC press, New York, USA, 2012, pp. 1–21 (Chapter 13).

[53] A. Laukkanen, K. Holmberg, H. Ronkainen, G. Stachowiak, P. Podsiadlo, W. Wolski, M. Gee, C. Gachot, L. Li, Topographical orientation effects on surface stresses influencing on wear in sliding DLC contacts, Part 2: modelling and simulations, Wear 388–389 (2017) 18–28.

[54] K. Holmberg, A. Laukkanen, A. Ghabchi, M. Rombouts, E. Turunen, R. Waudby, T. Suhonen, K. Valtonen, E. Sarlin, Computational modelling based wear resistance analysis of thick composite coatings, Tribol. Int. 72 (2014) 13–30.

[55] K. Holmberg, A. Laukkanen, E. Turunen, T. Laitinen, Wear resistance optimisation of composite coatings by computational microstructural modelling and simulation, Surf. Coating. Technol. 247 (2014) 1–13.

[56] B.N.J. Peterson, W.O. Winer, Wear Control Handbook, ASME, New York, USA, 1980.

[57] Y. Liu, S. Liu, W. Hild, J. Luo, J.A. Schaefer, Friction and adhesion in boundary lubrication measured by microtribometers, Tribol. Int. 39 (2006) 1674–1681.

[58] H. Abdullah Tasdemir, M. Wakayama, T. Tokoroyama, H. Kousaka, N. Umehara, Y. Mabuchi, T. Higuchi, Ultra-low friction of tetrahedral amorphous diamond-like carbon (ta-C DLC) under boundary lubrication in poly alpha-olefin (PAO) with additives, Tribol. Int. 65 (2013) 286–294.

[59] S. Miyake, M. Komiya, W. Kurosaka, Y. Matsumoto, Y. Saito, Y. Yasuda, Y. Okamoto, Boundary lubrication characteristic of metal-containing diamond-like carbon (DLC) films with poly alpha olefin (PAO) lubricant, Japanese Society of Tribologists, Tribol. Online 3 (2008) 310–315.

[60] A. Erdemir, C. Donnet, Tribology of diamondlike carbon films: current status and future prospects, J. Phys. Appl. Phys. 39 (2006) R311–R327.

[61] S. Cha, A. Erdemir (Eds.), Coating Technology for Vehicle Applications, Springer Verlag, Heidelberg, Germany, 2015.

[62] A. Rosenkranz, H.L. Costa, M.Z. Baykara, A. Martini, Synergetic effects of surface texturing and solid lubricants to tailor friction and wear – a review, Tribol. Int. 155 (2021) 106792.

[63] H. Ronkainen, S. Varjus, K. Holmberg, Friction and wear properties in dry, water- and oil lubricated DLC against alumina and DLC against steel contacts, Wear 222 (1998) 120–128.

[64] Anton Paar, Pin-on-disk Tribometer TRB3, 15.6.2021, https://www.anton-paar. com/kr-en/products/details/trb3-pin-on-disk-tribometer/.

[65] B. Bhushan, Principles and Applications in Tribology, John Wiley & Sons, New York, 1999.

[66] T. Zolper, L. Zhong, C. Chen, M. Jungk, T. Marks, Y. Chung, Q. Wang, Lubrication properties of polyalphaolefin and polysiloxane lubricants: molecular structure–tribology relationships, Tribol. Lett. 48 (2012) 355–365.

[67] Machinery Lubricants, Polyalphaolefin (PAO) lubricants explained, 15.6.2021, http s://www.machinerylubrication.com/Read/31106/polyalphaolefin-pao-lubricants, 15.6.2021.

[68] C. Donnet, J. Fontaine, A. Grill, T. Le Mogne, The role of hydrogen on the friction mechanism of diamond-like carbon films, Tribol. Lett. 9 (2001) 137–142.

[69] A. Erdemir, The role of hydrogen in tribological properties of diamond-like carbon films, Surf. Coating. Technol. 146–147 (2001) 292–297.

[70] J. Fontaine, C. Donnet, A. Grill, T. Le Mogne, Tribochemistry between hydrogen and diamond-like carbon films, Surf. Coating. Technol. 146–147 (2001) 286–291.

[71] S. Field, M. Jarratt, D. Teer, Tribological properties of graphite-like and diamond-like carbon coatings, Tribol. Int. 37 (2004) 949–956.

[72] K. Topolovec-Miklozic, F. Lockwood, H. Spikes, Behaviour of boundary lubricating additives on DLC coatings, Wear 265 (2008) 1893–1901.

[73] J. Stallard, D. Mercs, M. Jarratt, D. Teer, P. Shipway, A study on the tribological behaviour of three carbon-based castings, tested in air, water and oil environment at high loads, Surf. Coating. Technol. 177–178 (2004) 545–551.

[74] V. Bellido-Gonzalez, J. Hampshire, A. Jones, T. Allen, J. Witts, D. Teer, B. Pierret, Advances in the analysis and characterization of DLC coatings, Surf. Coating. Technol. 98 (1998) 1272–1279.